



**Northern Alberta Mosaic of
RADARSAT-1 Principal
Components Images Derived
from S1/S7
Ascending/Descending
Imagery**

**Northern Alberta Mosaic of
RADARSAT-1 Principal
Components Images Derived
from S1/S7
Ascending/Descending
Imagery**

E.C. Grunsky

Alberta Geological Survey

November 2002

©Her Majesty the Queen in Right of Alberta, 2002

The Alberta Energy and Utilities Board/Alberta Geological Survey (EUB/AGS) and its employees and contractors make no warranty, guarantee or representation, express or implied, or assume any legal liability regarding the correctness, accuracy, completeness or reliability of this publication. Any digital data and software supplied with this publication are subject to the licence conditions (specified in 'Licence Agreement for Digital Products'). The data are supplied on the understanding that they are for the sole use of the licensee and will not be redistributed in any form, in whole or in part, to third parties. Any references to proprietary software in the documentation, and/or any use of proprietary data formats in this release, do not constitute endorsement by the EUB/AGS of any manufacturer's product.

If this product is an EUB/AGS Special Report, the information is provided as received from the author and has not been edited for conformity to EUB/AGS standards.

When using information from this publication in other publications or presentations, due acknowledgment should be given to the EUB/AGS. The following reference format is recommended:

Grunsky, E.C. (2002): Northern Alberta mosaic of RADARSAT-1 principal components images derived from S1/S7 ascending/descending imagery; Alberta Energy and Utilities Board, EUB/AGS Geo-Note 2002-24.

Published November 2002 by:
Alberta Energy and Utilities Board
Alberta Geological Survey
4th Floor, Twin Atria Building
4999 – 98th Avenue
Edmonton, Alberta
T6B 2X3

Tel: (780) 422-3767 (Information Sales)
Fax: (780) 422-1918

Web site: www.ags.gov.ab.ca

1 Introduction

This investigation uses RADARSAT-1 standard beam imagery as a tool for mapping surficial geology and geological structures in northern Alberta. Between 1999 and 2002, the Alberta Geological Survey acquired RADARSAT-1 imagery for northern Alberta north of 55° latitude. They were then processed to obtain orthorectified, tiled and filtered images for its regional mapping program and for future applications in other areas of environmental and resource management. From September to December 1999, 280 scenes of RADARSAT-1 Standard Beam modes S1 and S7 were captured for ascending and descending passes, as shown in Figures 1 to 4. The autumn season was chosen to minimize the effect of vegetation and maximize the microwave reflectance from the ground surface.

Radar imagery has been commonly used for mapping geomorphology and geological structure (Lowman et al., 1987; Singhroy et al., 1993; Gupta, 1991; Singhroy and Saint-Jean, 1999; Smith et al., 1999; Paganelli et al., 2001; Paganelli et al., 2002; Grunsky, *in press*). The range of incidence angles, all-weather atmospheric penetration and response to surface morphology give radar imagery significant advantages in measuring surface features relative to conventional, fixed-beam optical satellites. A review of RADARSAT-1 imagery in geoscience applications showed that most studies used individual radar images with a single incidence angle, polarization, frequency and resolution. However, radar imagery has also helped extract information from the integration of optical and geophysical imagery (Harris et al., 1994; Mustard, 1994). Masuoka et al. (1988) applied the technique of principal components analysis (PCA) on a radar image composite derived from Shuttle Imaging Radar (SIR-B) and Seasat. Although most studies use radar for delineating geological structure, it has also aided in mapping surficial geology (Graham and Grant, 1994).

Previous studies on the use of PCA with radar imagery (ERS-1 and Canada Centre for Remote Sensing (CCRS) C-SAR) found the technique useful for highlighting structural features in the Sudbury area of Ontario, Canada (Moon et al., 1994 and Harris et al., 1994). In the study by Moon et al. (1994), different incidence angles, look directions, frequencies and polarizations were able to highlight geological structure. This Geo-Note used two look directions and incidence angles; polarization and frequency were held constant.

The detection of geological structure is partially dependent on the look direction of the satellite (Harris, 1984; Lowman et al., 1987). If a linear feature is parallel to the look direction of a radar image, then it may be nearly invisible. Studies have indicated (e.g., Harris, 1984) that the linear features show up as distinctive lines in radar imagery when the feature is within 20 degrees of the perpendicular to the look direction of the radar sensor. In the case of using multi-beam imagery for RADARSAT-1 data, the identification of linear features will be determined by a range of look directions that are different for each beam mode.

The use of radar imagery in geological applications and projected use of RADARSAT-1 has been discussed by Singhroy et al. (1993). More recently, Singhroy and Saint-Jean (1999) have shown that variation in RADARSAT-1 incidence angles highlights ground features based on relief and surface texture. In this Geo-Note, the strategy of adopting S1 and S7 imagery was to contrast the radar responses based on the incidence angle and look direction (ascending-east looking/descending-west looking). The difference in responses due to the incidence angle is a potential indicator of surface variation. Figure 5 shows the configuration of beam modes and look direction for the image integration used for this study. Influences on the response are backscatter, which can be attributed to both volume and surface conditions, and these are influenced by topography, vegetation and surface moisture (Raney, 1998). The nature of backscatter, due to the variation of incidence angle, is likely to have an effect on the response. Lowman et al. (1987) described the effect of incidence angle on the ability to detect

Orthorectified Imagery
for RADARSAT-1
Beam Mode S1 Ascending

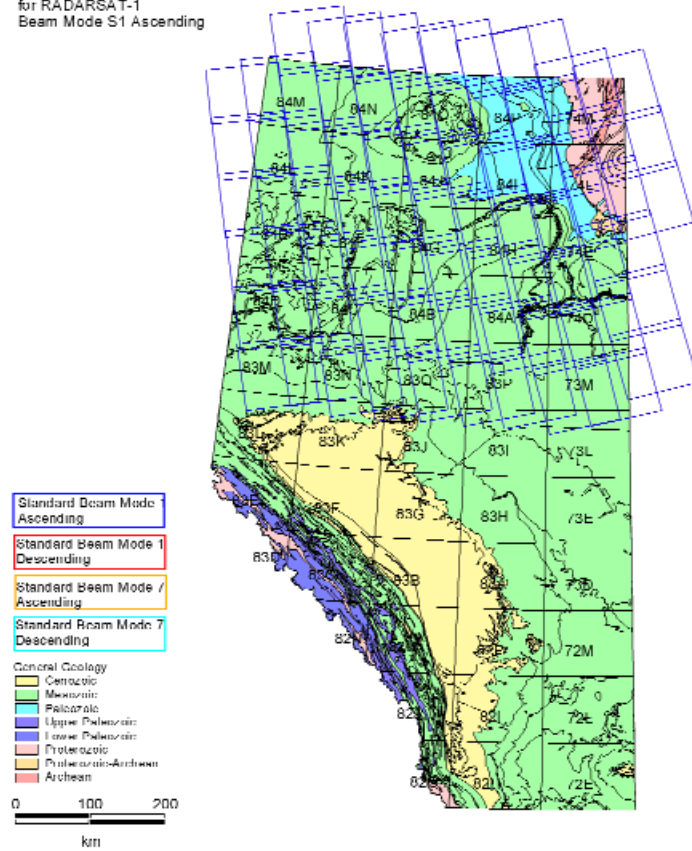


Figure 1. Standard Beam Mode 1 ascending coverage for northern Alberta.

Orthorectified Imagery
for RADARSAT-1
Beam Mode S1 Descending

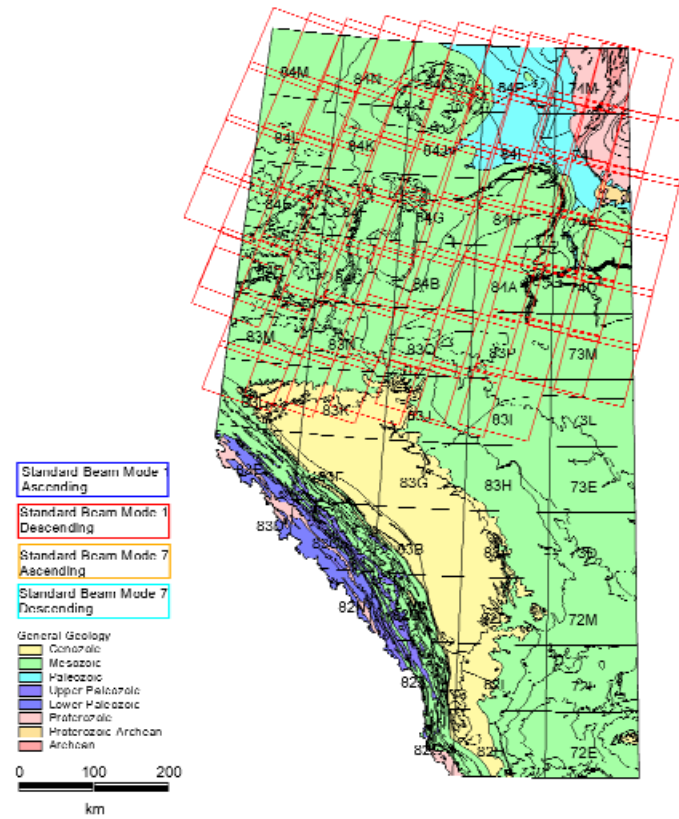


Figure 2. Standard Beam Mode 1 descending coverage for northern Alberta.

Orthorectified Imagery
for RADARSAT-1
Beam Mode S7 Ascending

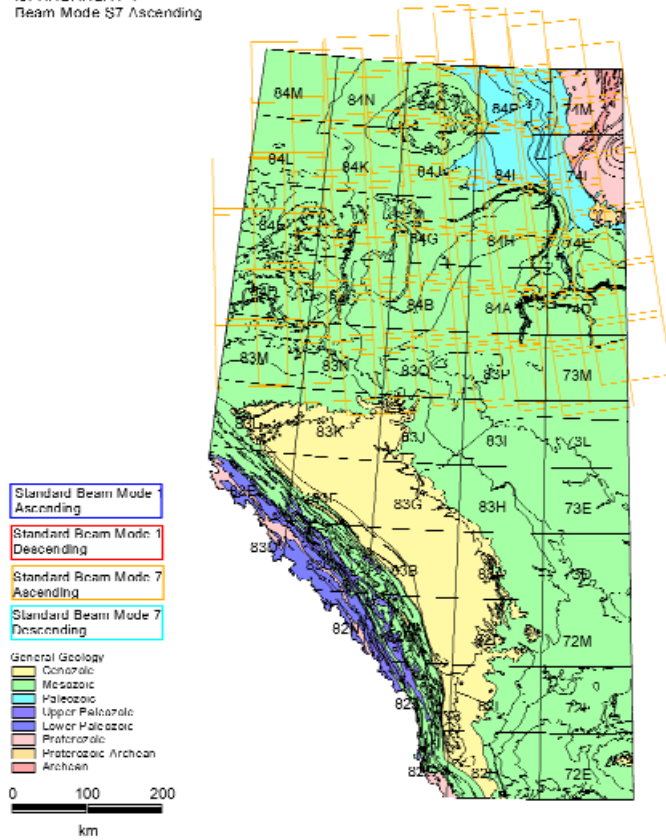


Figure 3. Standard Beam Mode 7 ascending coverage for northern Alberta.

Orthorectified Imagery
for RADARSAT-1
Beam Mode S7 Descending

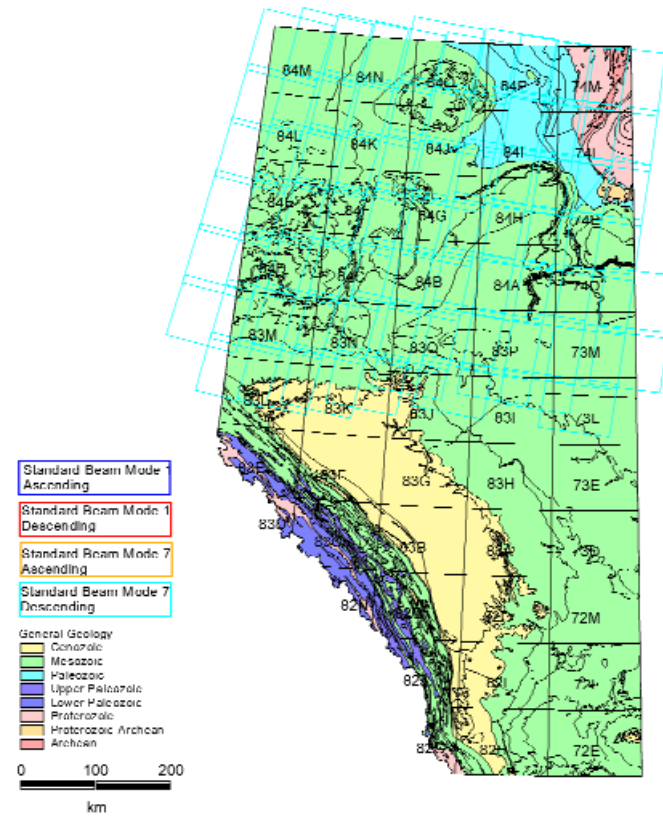


Figure 4. Standard Beam Mode 7 descending coverage for northern Alberta.

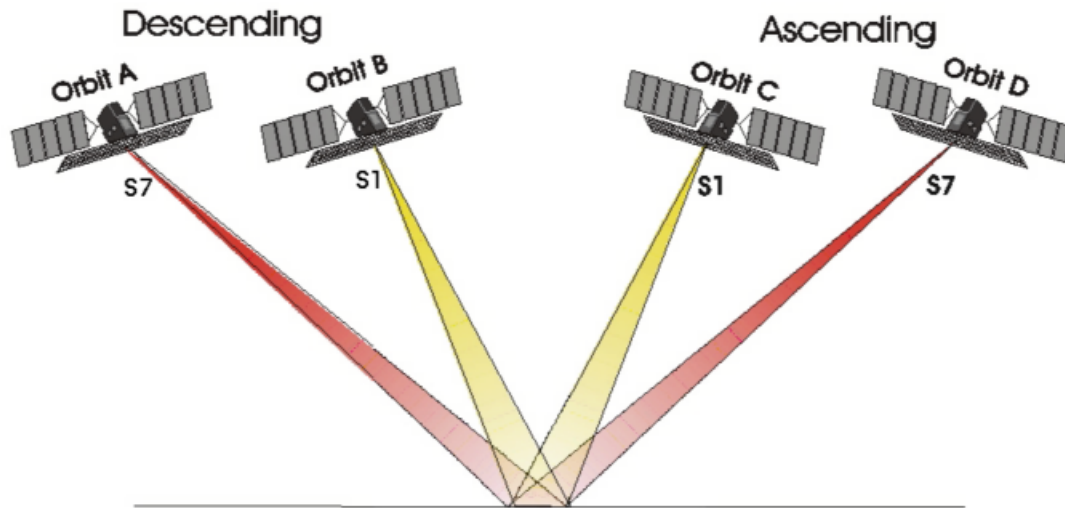


Figure 5. Multi-beam configuration of RADARSAT-1 S1 and S7 ascending/descending imagery.

differences in topography, where topography is expressed by shading controlled by local incidence angle variation. Incidence angles that are shallow (S1) are better suited for highlighting the differences in topography.

RADARSAT-1 image characteristics are summarized by Luscombe et al., 1993. The RADARSAT-1 satellite operates at a single microwave frequency of 5.3 GHz (5.6 cm wavelength), generally known as C-band radar. The microwave transmission operates in H-H polarization mode. The RADARSAT-1 Path Image (SGF) georeferenced images using a land-based lookup table provided by Radarsat International and the CCRS. Each Standard Beam image is a composite of four looks (Raney, 1998, p. 73). This composite increases the signal-to-noise ratio at the expense of the spatial resolution. The imagery was provided at a nominal resolution of 12.5 m (close to the single look spatial resolution), although the true spatial resolution of the averaged four-look image is closer to 25 m.

2 Image Acquisition

Image acquisition occurred between September and December 1999. Although the effects of weather patterns are negligible on the radar response, factors that will affect the response include the amount of surface moisture from significant rain events and the loss of leaves in the deciduous foliage. These effects will most likely cause some differences between scenes captured at different times. In this report, these effects have not been examined. However, it is unlikely these effects would mask variation in terrain morphology or features associated with geological structures. It is more likely the loss of foliage will increase the contrast in features associated with structure and geomorphology.

3 Satellite Image Processing Method

For processing multi-beam radar imagery, the images must be orthorectified to minimize the effects of the shortening and layover associated with the difference in incidence angles. In this study, S1 (20-27°) and S7 (45-49°) incidence angles require orthorectification so the differences in features are distinct from differences associated with layover and shortening. Orthorectification was carried out using digital elevation data provided by the Resource Data Division of the Alberta Department of Sustainable Development. The data were provided in a grid form at 100-metre resolution.

Multi-channel, remotely sensed imagery (multivariate data) contains responses that may reflect interactions between channels that are not visually obvious or are difficult to visualize from the individual source channels. However, a number of methods are suitable for enhancing contrast differences in measurements over geographic areas. For example, when two images are being compared, methods such as ratios or subtraction can be applied and can yield suitable contrasts. When three or more images are compared, contrasts become more complicated and multivariate techniques may be more appropriate. The method of PCA creates linear combinations of variables (channels) based on the covariance of the input channels and is commonly available with satellite image processing packages. The application of principal components is one method that can be used to discover interactions between the multi-channel data. Each successive principal component represents a linear combination of the input channels, which accounts for a portion of the overall variation of the data. The first principal component accounts for the most variation (by definition), followed by successively lower order components, which account for decreasing variation of the data. Each component can be viewed as a new variable (or channel) that describes relationships of the original variables in the form of linear combinations. Discussions on the use of PCA can be found in Richards (1986) and Gupta (1991).

Currently, 25 NTS areas (73M, 74D, 74E, 74L, 74M, 83M, 83N, 83O, 83P, 84A, 84B, 84C, 84D, 84E, 84F, 84G, 84H, 84I, 84J, 84K, 84L, 84M, 84N, 84O and 84P) have been tiled from the orthorectified imagery. Grunsky (*in press*) has shown that features depicting geomorphology and geological structure can be extracted from multi-beam RADARSAT-1 imagery in NTS areas 74L and 74E.

4 Mosaic Composition

The northern Alberta mosaic has been assembled using four each of the four principal components over the 25 tiled NTS areas. The imagery has been re-sampled to 100-metre resolution and is available in three projections: UTM Zones 11 and 12, and 10 degree Transverse Mercator projection with a central meridian of 115 degrees west. The datum used for all three projections is the North American Datum of 1983 (NAD83).

The images have been created in geoTIFF format, which has the georeferencing information imbedded in the image so it can be loaded into a variety of GIS and image processing software packages. The geoTIFF images are included with this Geo-Note and are described in the following tables.

Table 1. GeoTiff files on CD 1: 10 degree Transverse Mercator projection with a central meridian of 115 degrees west (NAD83)

| File Name | Description |
|--|----------------------------------|
| northern_composite_PC123_100m_10tm_n83.tif | Principal components 1, 2, and 3 |
| northern_composite_PC124_100m_10tm_n83.tif | Principal components 1, 2, and 4 |
| northern_composite_PC134_100m_10tm_n83.tif | Principal components 1, 3, and 4 |
| northern_composite_PC1_100m_10tm_n83.tif | Principal component 1 |
| northern_composite_PC234_100m_10tm_n83.tif | Principal components 2, 3, and 4 |
| northern_composite_PC2_100m_10tm_n83.tif | Principal component 2 |
| northern_composite_PC3_100m_10tm_n83.tif | Principal component 3 |
| northern_composite_PC4_100m_10tm_n83.tif | Principal component 4 |

Table 2. GeoTiff files on CD 2: UTM projection, Zone 11 (NAD83)

| File Name | Description |
|---|----------------------------------|
| northern_composite_PC123_100m_utm11_n83.tif | Principal components 1, 2, and 3 |
| northern_composite_PC124_100m_utm11_n83.tif | Principal components 1, 2, and 4 |
| northern_composite_PC134_100m_utm11_n83.tif | Principal components 1, 3, and 4 |
| northern_composite_PC1_100m_utm11_n83.tif | Principal component 1 |
| northern_composite_PC234_100m_utm11_n83.tif | Principal components 2, 3, and 4 |
| northern_composite_PC2_100m_utm11_n83.tif | Principal component 2 |
| northern_composite_PC3_100m_utm11_n83.tif | Principal component 3 |
| northern_composite_PC4_100m_utm11_n83.tif | Principal component 4 |

Table 3. GeoTiff files on CD 3: UTM projection, Zone 12 (NAD83)

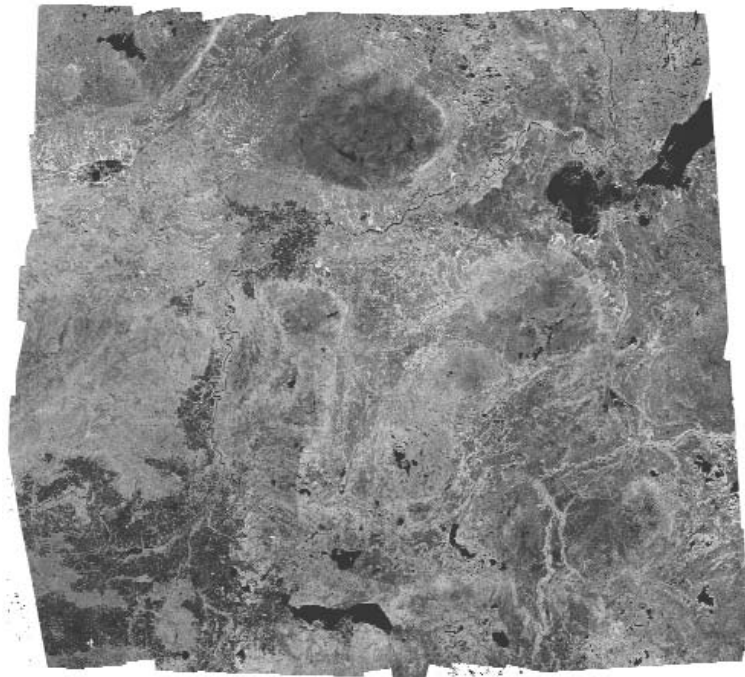
| File Name | Description |
|---|----------------------------------|
| northern_composite_PC123_100m_utm12_n83.tif | Principal components 1, 2, and 3 |
| northern_composite_PC124_100m_utm12_n83.tif | Principal components 1, 2, and 4 |
| northern_composite_PC134_100m_utm12_n83.tif | Principal components 1, 3, and 4 |
| northern_composite_PC1_100m_utm12_n83.tif | Principal component 1 |
| northern_composite_PC234_100m_utm12_n83.tif | Principal components 2, 3, and 4 |
| northern_composite_PC2_100m_utm12_n83.tif | Principal component 2 |
| northern_composite_PC3_100m_utm12_n83.tif | Principal component 3 |
| northern_composite_PC4_100m_utm12_n83.tif | Principal component 4 |

5 References

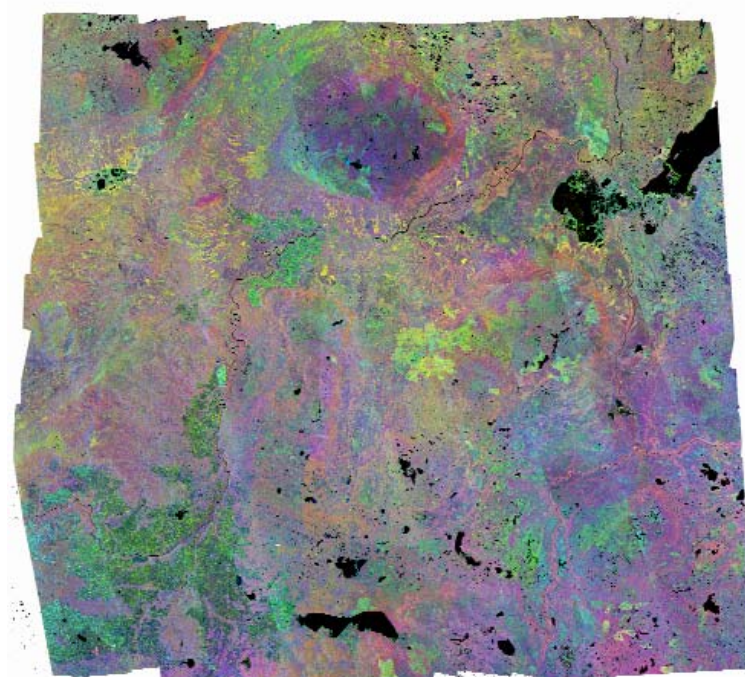
- Graham, D.F., and Grant, D.R., (1994): Airborne SAR for Surficial Geologic Mapping, *Canadian Journal of Remote Sensing*, Special Issue on Radar Geology, v.1. 20, no. 3, p.319-323.
- Grunsky, E. C., (in press): The Application of Principal Components Analysis to Multi-beam RADARSAT-1 Satellite Imagery – A Tool for Land Cover and Terrain Mapping, *Canadian Journal of Remote Sensing*
- Gupta, R.P., (1991): *Remote Sensing Geology*, Springer-Verlag, New York, 356 p.
- Harris, J., (1984): Lineament Mapping of Central Nova Scotia Using Landsat-MSS and SEASAT-SAR Imagery, Proceedings of the 9th Canadian Symposium on Remote Sensing, St. John's, Newfoundland, p. 359-373.
- Harris, J.R., Bowie, C., Rencz, A.N., and Graham, D., (1994): Computer Enhancement Techniques for the Integration of Remotely Sensed, Geophysical, and Thematic Data for the Geosciences, *Canadian Journal of Remote Sensing*, v. 20, no. 3, p. 210-221.
- Luscombe, A.P., Feguson, I., Shepherd, N., Zimcik, D.G., and Naraine, P., (1993): The RADARSAT Synthetic Aperture Radar Development, , *Canadian Journal of Remote Sensing*, Special Issue RADARSAT, Vol. 19, no. 4, p.298-310.
- Lowman, P.D., Harris, J., Masuoka, P.M., Singhroy, V.H. and Slaney, V.R., (1987): Suttle Imaging Radar 9SIR-B) Investigations of the Canadian Shield: Initial Report, *IEEE Transactions on Geoscience and Remote Sensing*, v. GE-25, no., January, 1987, p. 55-66.
- Masuoka, P.M., Harris, J., Lowman, P.D. and Blodget, H.W., (1988): Digital Processing of Orbital Radar Data to Enhance Geologic Structure: Examples from the Canadian Shield, *Photogrammetric Engineering and Remote Sensing*, v. 54, no. 5, May 1988, p. 621-632.

- Moon, W.M., Won, J.S., Singhroy, V., Lowman, P.D., (1994): ERS-1 and CCRS C-SAR Data Integration for Look-Direction Bias Correction using Wavelet Transform, Canadian Journal of Remote Sensing, Special Issue on Radar Geology, v. 20, no. 3, p. 280-285.
- Mustard, J.F., (1994): Lithologic Mapping of Gabbro and Periodotite Sills in the Cape Smith Fold and Thrust Belt with Thematic Mapper and Airborne Radar Data, Canadian Journal of Remote Sensing, Special Issue on Radar Geology, v. 20, no. 3, p.222-232.
- Paganelli, F., Grunsky, E.C., and Richards, J.P., (2002): RADARSAT-1 Principal Component Imagery: a case study in the Buffalo Head Hills area, northern central Alberta, Canadian Journal of Remote Sensing.
- Paganelli, F., Grunsky, E.C., and Richards, J.P., (2001): Structural Interpretation of Radarsat and Landsat7 TM Images for Kimberlite Exploration in the Buffalo Head Hills Area, North-central Alberta, 10th Annual Calgary Mining Forum - Alberta Geological Survey Minerals Section Open House, April 18-19, 2001, Calgary, Alberta.
- Raney, K.R., (1998): Radar Fundamentals: Technical Perspective, in: Manual of Remote Sensing: Principles and Applications of Imaging Radar, 3rd edition v. 2, John Wiley & Sons, p 9-130.
- Richards, J.A., (1986): Remote Sensing Digital Image Analysis, Springer-Verlag, New York, 281 p.
- Singhroy, V., Slaney, R., Lowman, P, Harris, J. and Moon, W., (1993): Radarsat and Radars Geology in Canada, Canadian Journal of Remote Sensing, Special Issue RADARSAT, v. 19, no. 4, p.338-351.
- Singhroy, V., Saint-Jean, R., (1999): Effects of Relief on the Selection of RADARSAT-1 Incidence Angle for Geological Applications, Canadian Journal of Remote Sensing, v. 25, no. 3, p. 211-217.
- Smith S.K., Grieve, R.A.F., Harris, J.R. and Singhroy, V., (1999): The Utilization of RADARSAT-1 Imagery for the Characterization of Terrestrial Impact Landforms, Canadian Journal of Remote Sensing, v. 25, no. 3, p. 218-228.

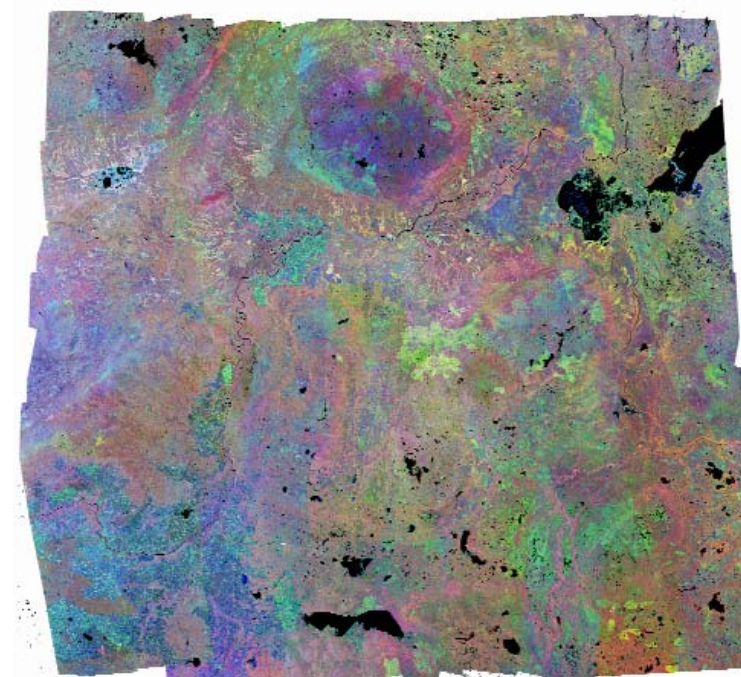
Table 1 pictures of GeoTiff files on CD 1: 10 degree Transverse Mercator projection with a central meridian of 115 degrees west (NAD83) for visual use only. The Tiff files are intended to be used in a geographic information system or spatial image processing package.



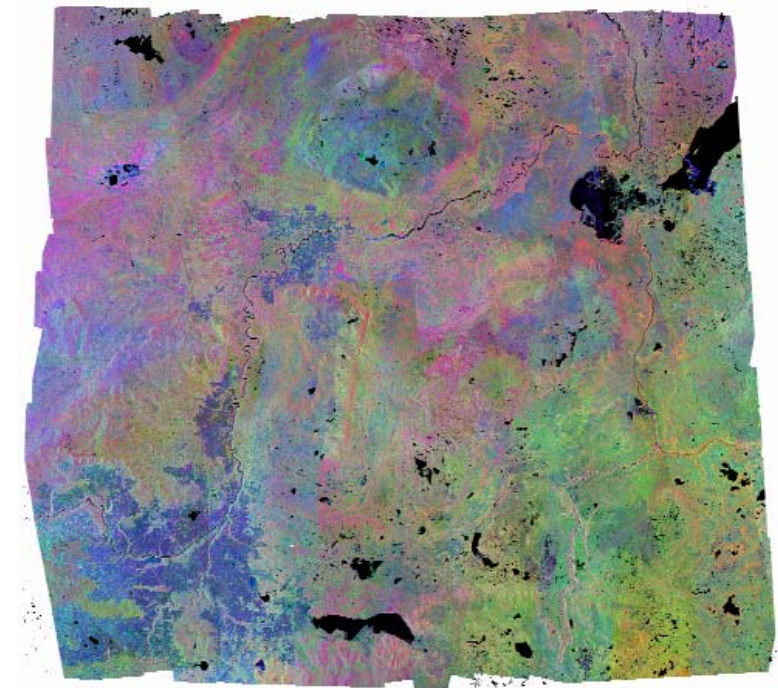
northern_composite_PC1_100m_10tm_n83.tif



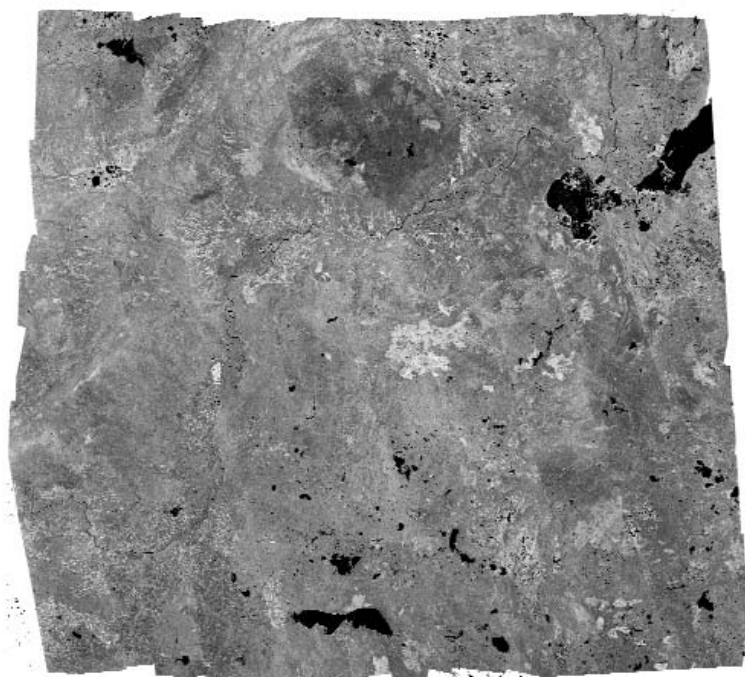
northern_composite_PC123_100m_10tm_n83.tif



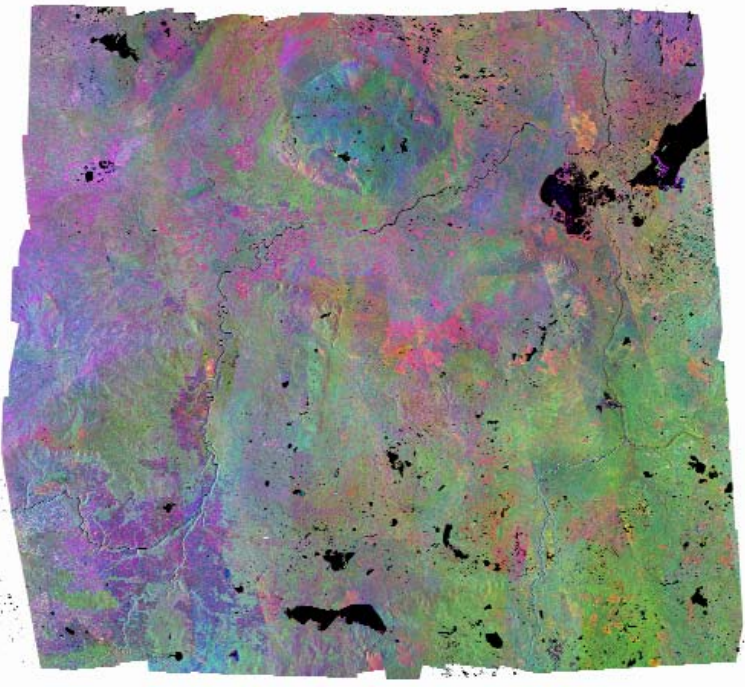
northern_composite_PC124_100m_10tm_n83.tif



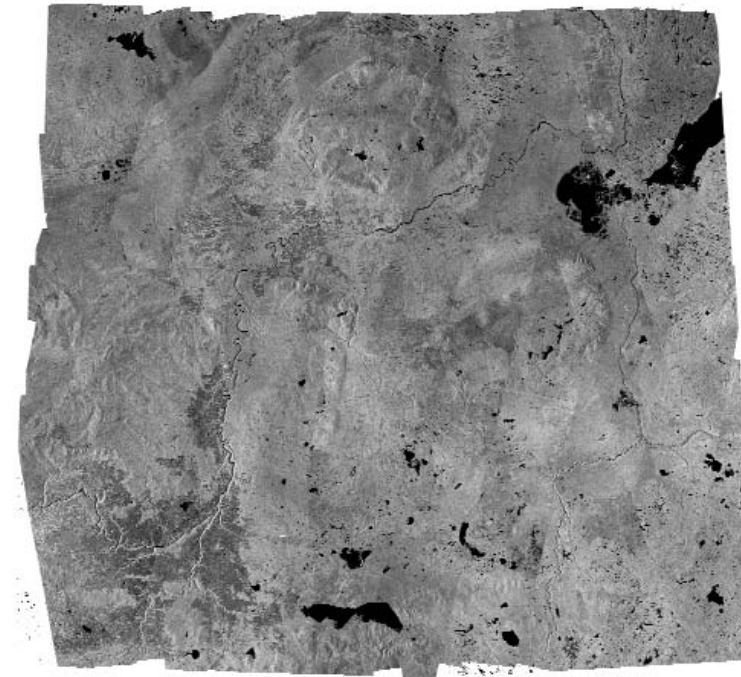
northern_composite_PC134_100m_10tm_n83.tif



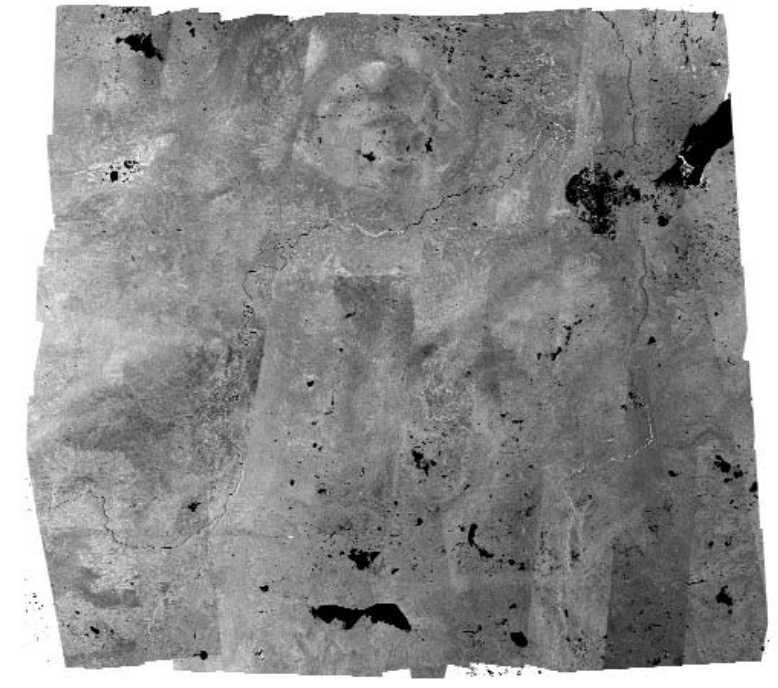
northern_composite_PC2_100m_10tm_n83.tif



northern_composite_PC234_100m_10tm_n83.tif

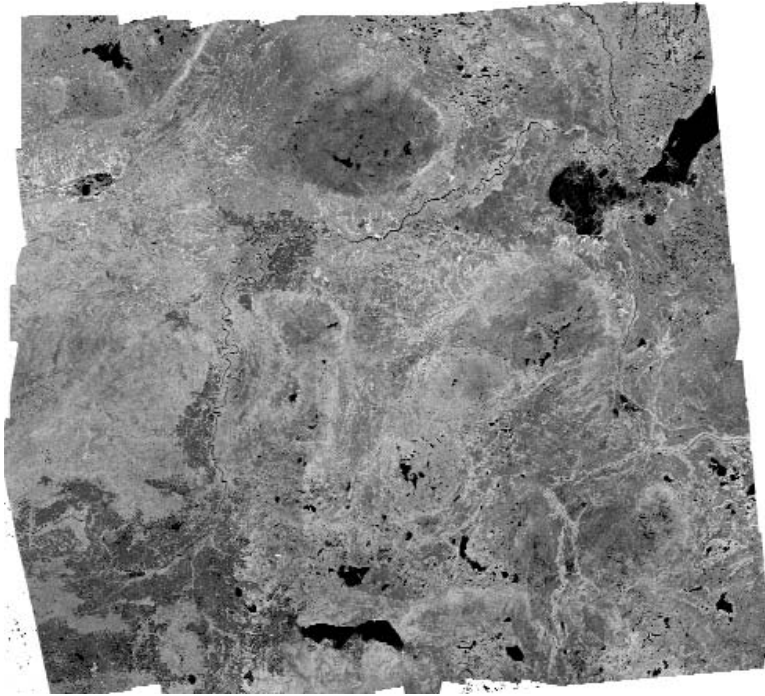


northern_composite_PC3_100m_10tm_n83.tif

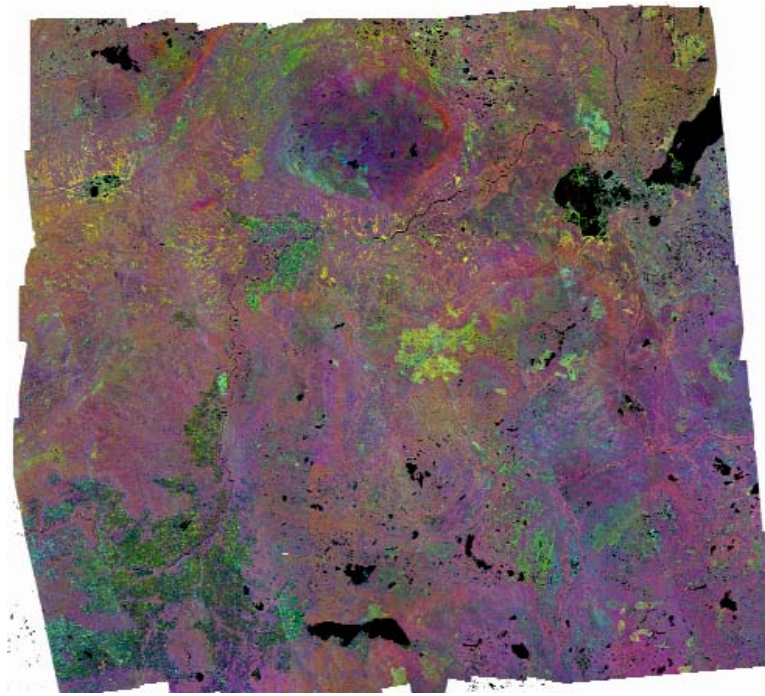


northern_composite_PC4_100m_10tm_n83.tif

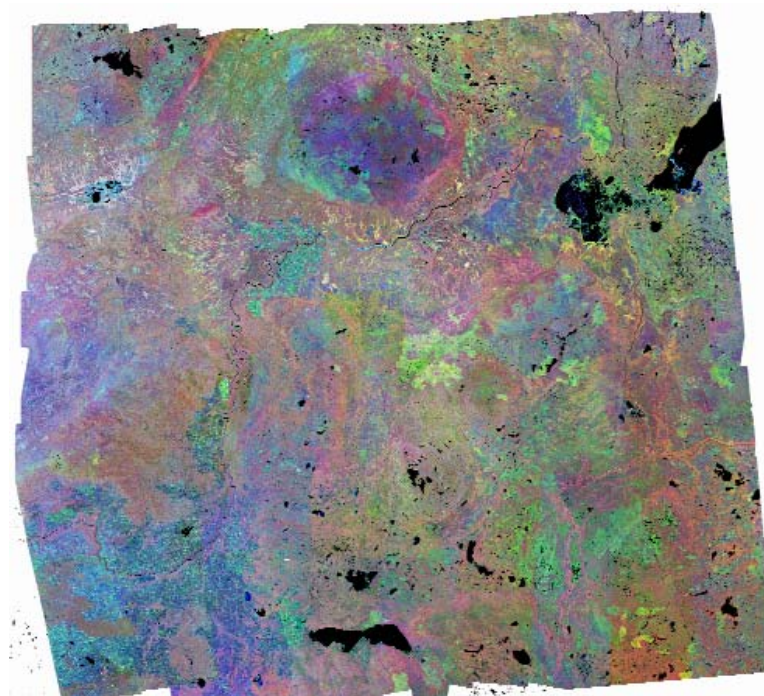
Table 2 pictures of GeoTiff files on CD 2: UTM projection, Zone 11 (NAD83 for visual use only. The Tiff files are intended to be used in a geographic information system or spatial image processing package.



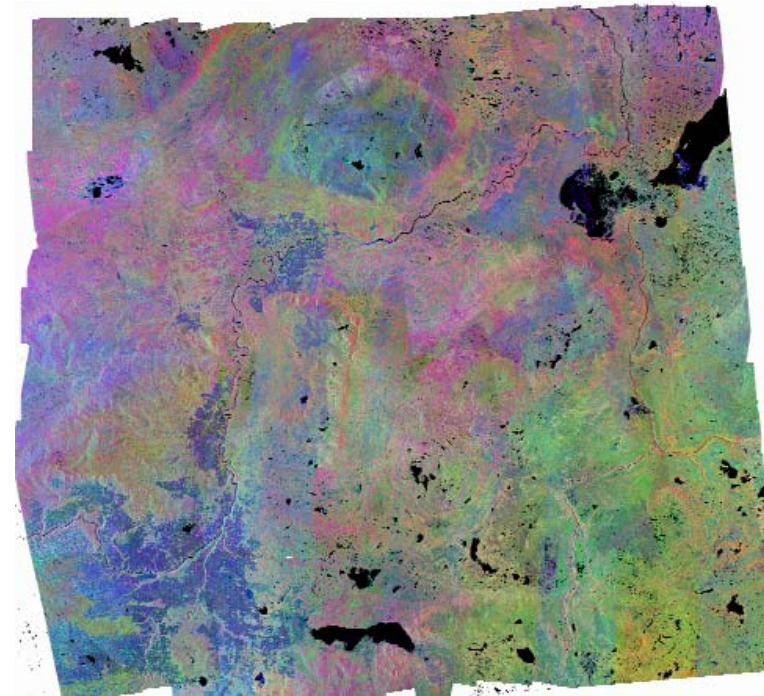
northern_composite_PC1_100m_utm11_n83.tif



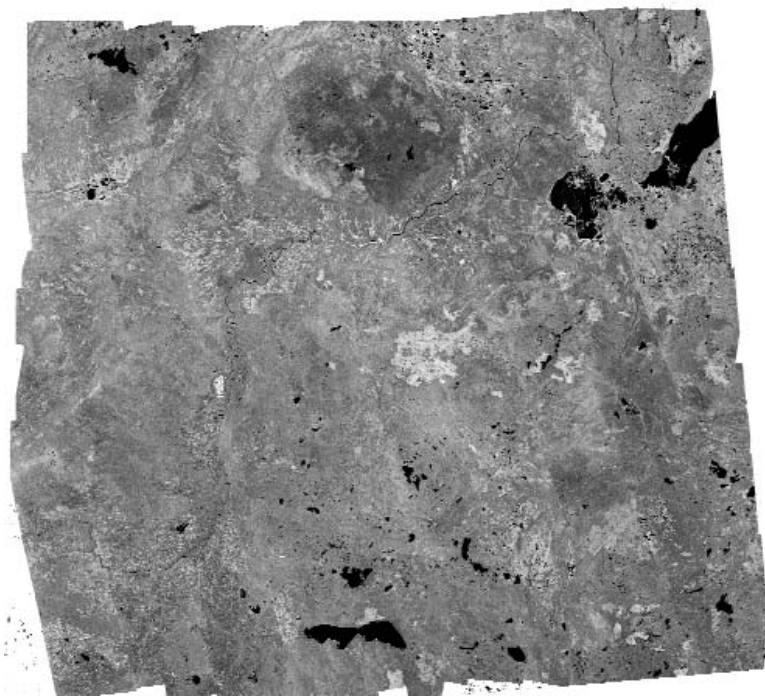
northern_composite_PC123_100m_utm11_n83.tif



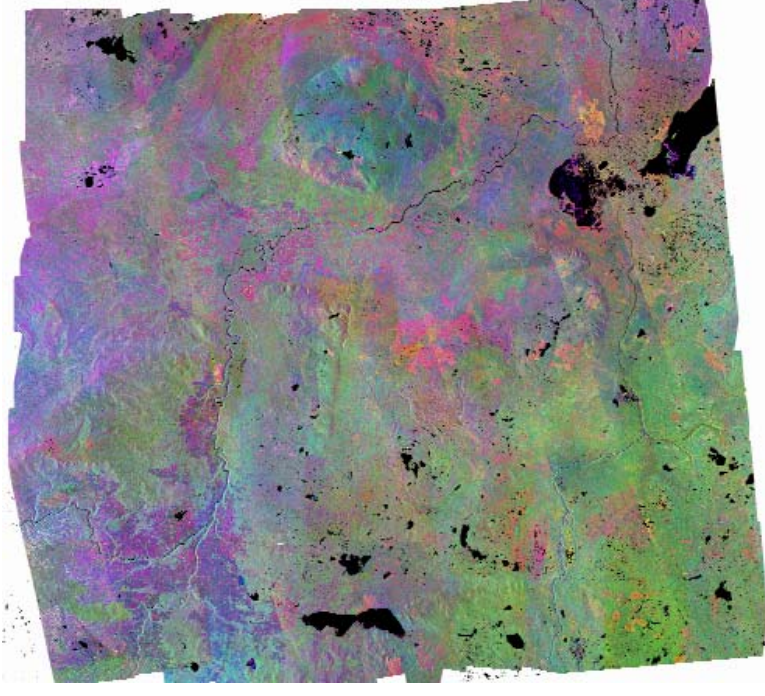
northern_composite_PC124_100m_utm11_n83.tif



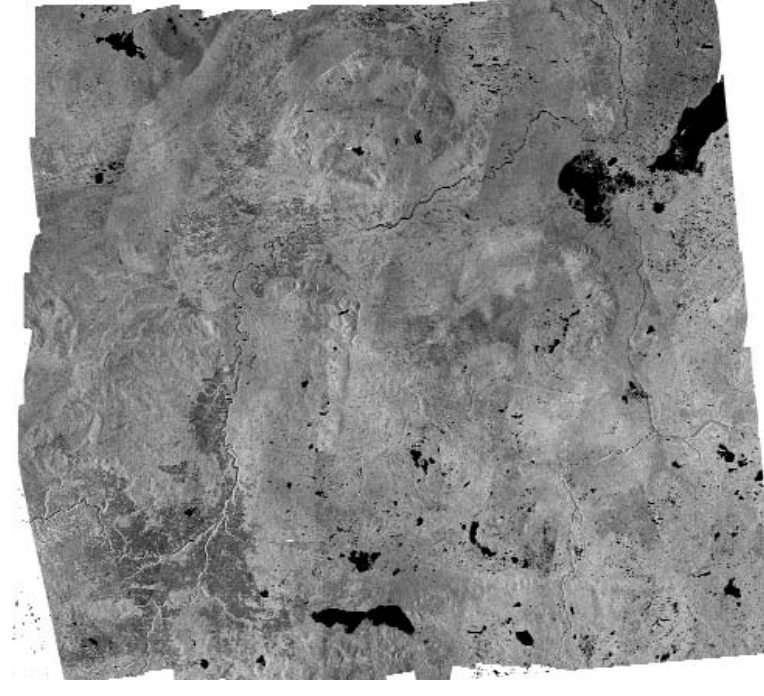
northern_composite_PC134_100m_utm11_n83.tif



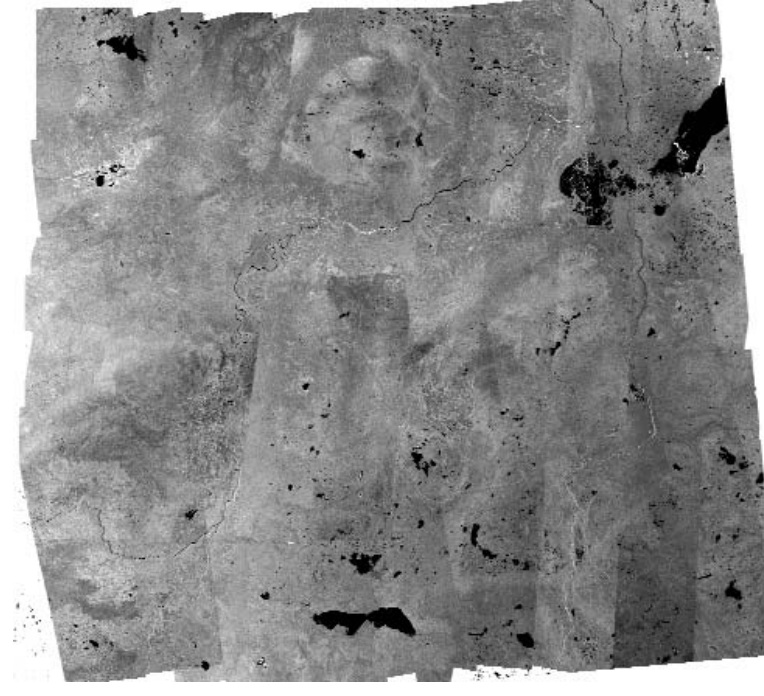
northern_composite_PC2_100m_utm11_n83.tif



northern_composite_PC234_100m_utm11_n83.tif

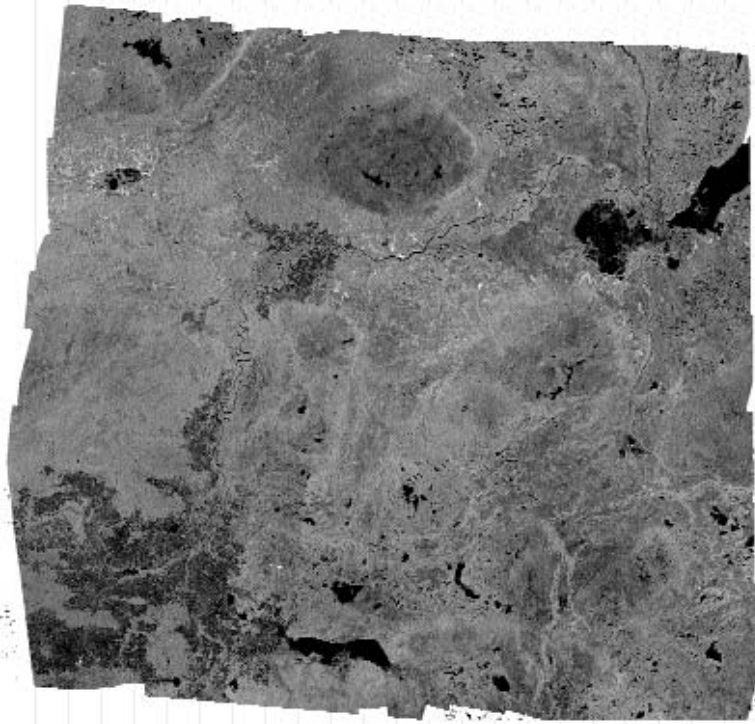


northern_composite_PC3_100m_utm11_n83.tif

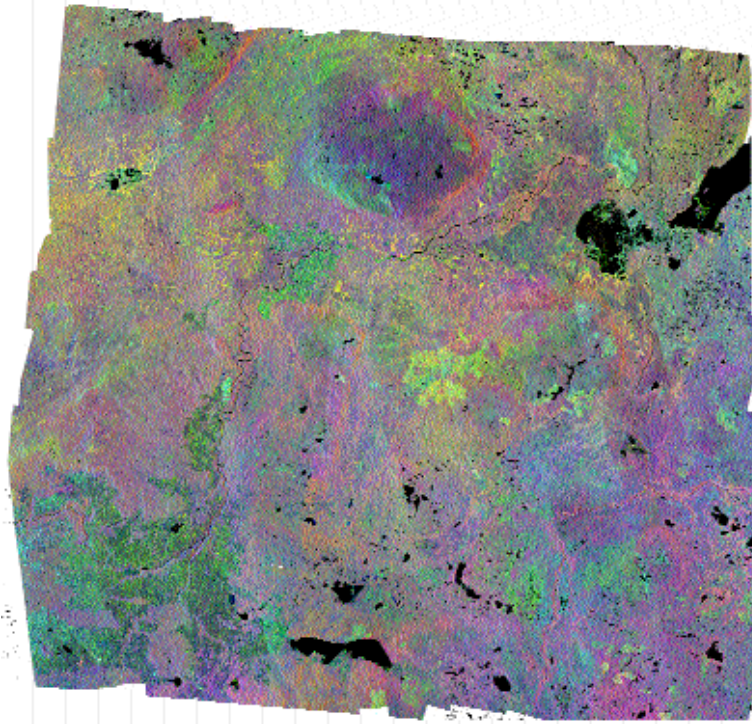


northern_composite_PC4_100m_utm11_n83.tif

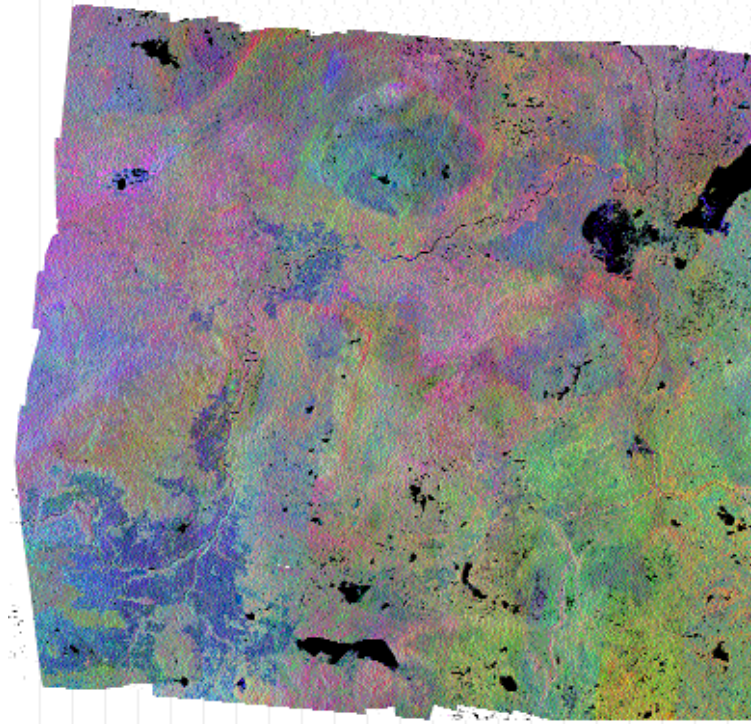
Table 3 pictures of GeoTiff files on CD 3: UTM projection, Zone 12 (NAD83) for visual use only. The Tiff files are intended to be used in a geographic information system or spatial image processing package.



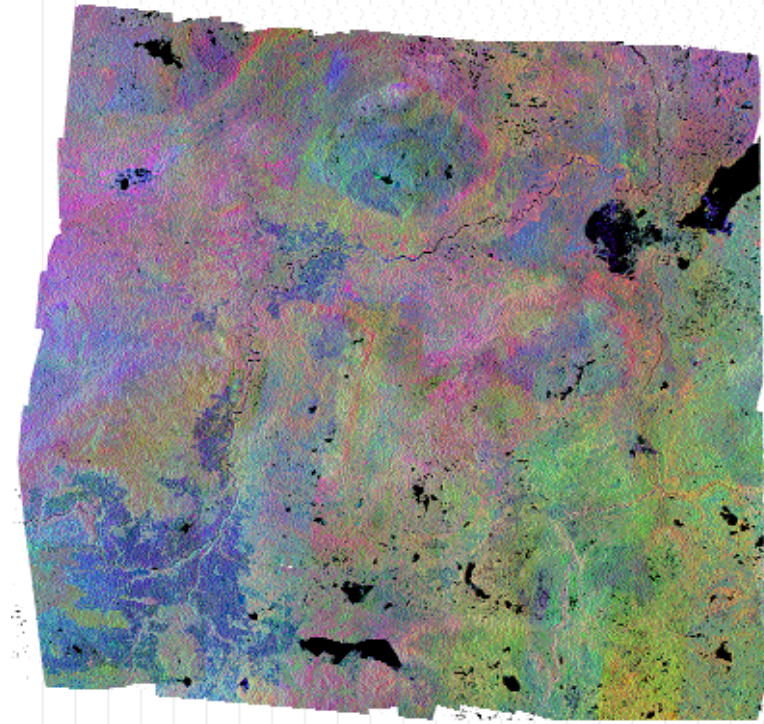
northern_composite_PC1_100m_utm12_n83.tif



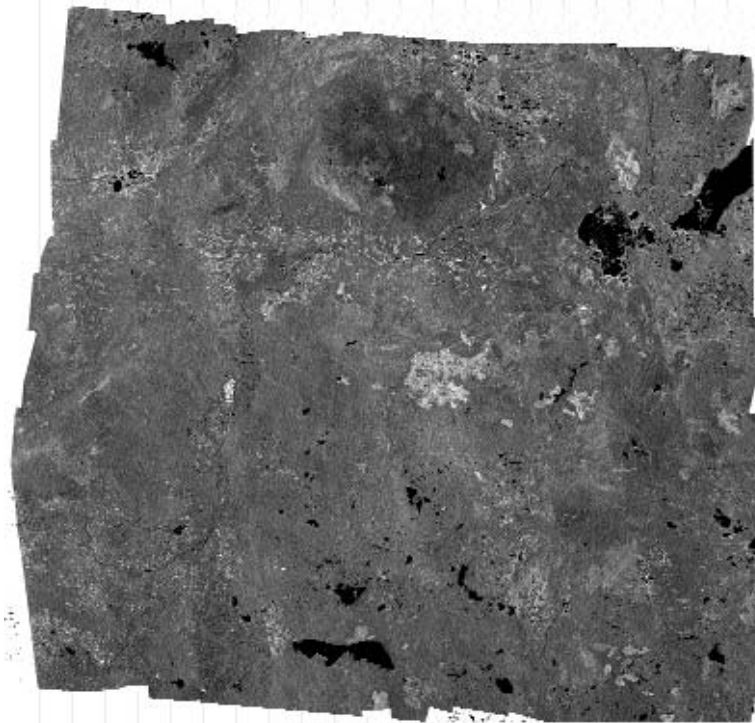
northern_composite_PC123_100m_utm12_n83.tif



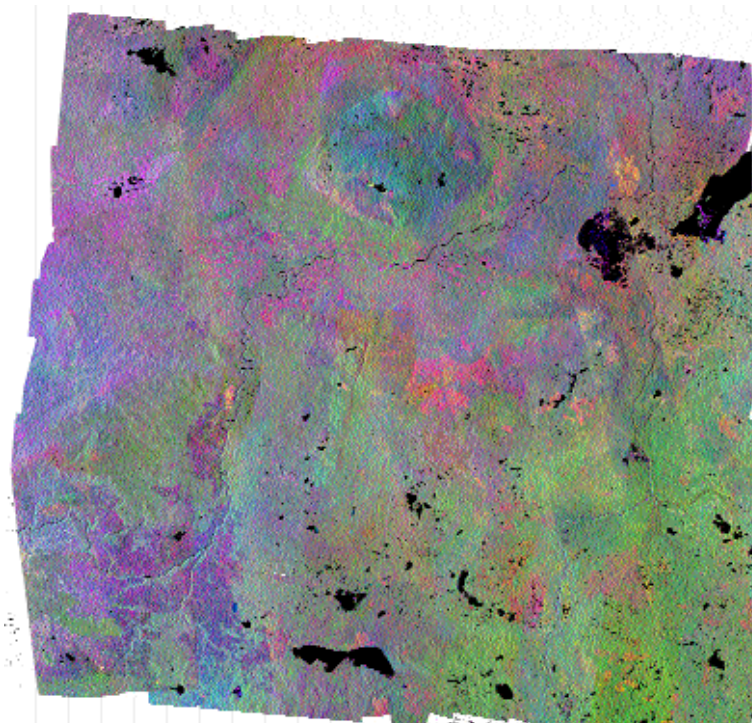
northern_composite_PC124_100m_utm12_n83.tif



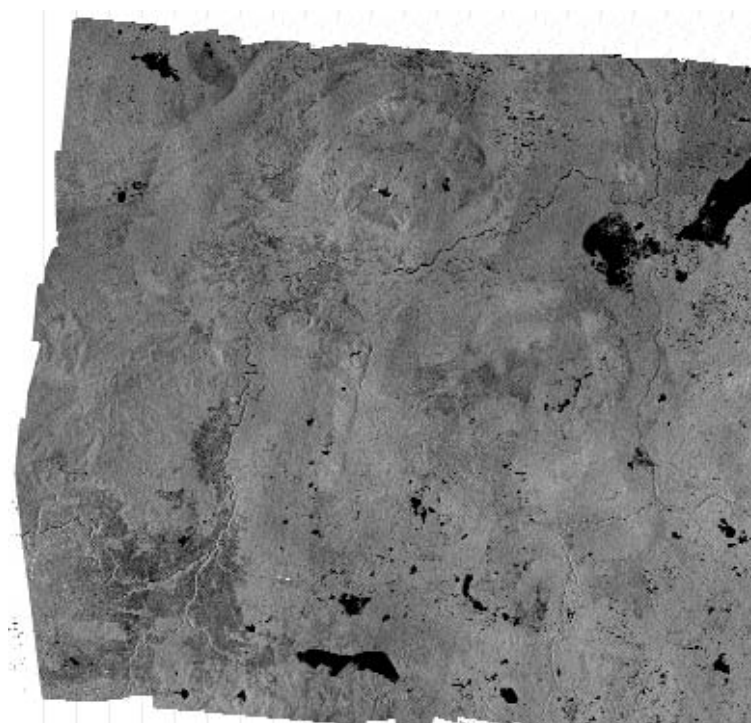
northern_composite_PC134_100m_utm12_n83.tif



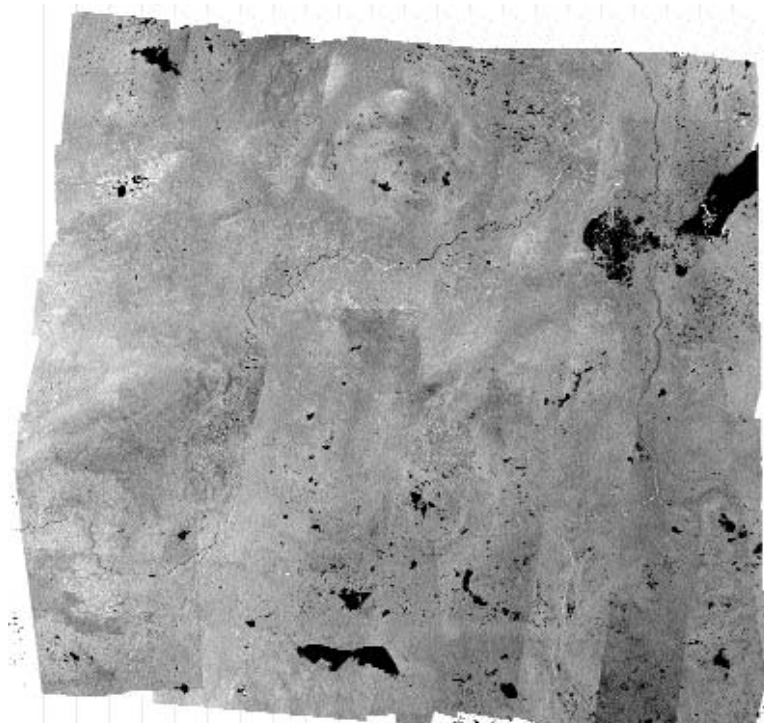
northern_composite_PC2_100m_utm12_n83.tif



northern_composite_PC234_100m_utm12_n83.tif



northern_composite_PC3_100m_utm12_n83.tif



northern_composite_PC4_100m_utm12_n83.tif